

Synthesis and Characterization of Ge Nanoclusters in Amorphous GeO_x (x~0.1) Nano-Films Grown by Magnetron Sputtering

Javier Sotelo Medina
Programa en Nanociencias y
Nanotecnología
CINVESTAV, IPN
Ciudad de México, México
javier.sotelo@cinvestav.mx

Daniel Ortiz Gutiérrez
Departamento de Ingeniería
Eléctrica, Sección de Electrónica
y Estado Sólido (DIE-SEES)
CINVESTAV, IPN
Ciudad de México, México
dotizg@cinvestav.mx

Vyacheslav Elyukhin
Departamento de Ingeniería
Eléctrica, Sección de Electrónica
y Estado Sólido (DIE-SEES)
CINVESTAV, IPN
Ciudad de México, México
elyukhin@cinvestav.mx

Ramón Peña Sierra
Departamento de Ingeniería
Eléctrica, Sección de Electrónica
y Estado Sólido (DIE-SEES)
CINVESTAV, IPN
Ciudad de México, México
rpsierra@cinvestav.mx

Abstract— We investigated how the processing condition of the amorphous Ge (α -Ge) nano-films (growth technique, substrate temperature, annealing conditions and the processing atmosphere composition) influence on their physical-chemical properties. Ge clusters or quantum dots (QDs) in α -Ge nano-films were prepared by a combined process comprising the magnetron sputtering technique and a post-grown annealing stage at 800 K for 3.5 hours in a reducing atmosphere. The α -Ge nano-films were grown in the temperature range from 300 to 800 K. Secondary ion mass spectrometry (SIMS) analysis shown an oxygen content of $3.5 \times 10^{21} \text{ cm}^{-3}$ in the films fixed by operative conditions of the sputtering system. The electrical characterization shown that the samples grown at room temperature resulting insulating, while the samples grown at temperatures over 500 K have n-type conductivity with electron concentration of $3.5 \times 10^{19} \text{ cm}^{-3}$, in average. The optical transmittance and photoluminescence characterization demonstrated that the films have an optical band gap (E_g) of 1.2 eV, generated by the presence of Ge nanoclusters in the α -GeO_x nano-films. The process used in this work demonstrated their potential to nucleate Ge clusters with sizes from 1 to 8 nm in an amorphous matrix, as was proven by X-ray diffraction (XRD) and Raman scattering measurements.

Keywords—Germanium nanoparticles, clusters, amorphous GeO_x, ordered nanostructures, magnetron sputtering, XRD characterization, Raman scattering and photoluminescence.

I. INTRODUCTION

New generations of solar cells based on intermediate band heterojunctions with quantum effects produced by embedded nanocrystals (Quantum Dots, QDs) have attracted the interest of scientists around the world due to the generation of two or more excitons from a single photon, Multiple Exciton Generation (MEG) effect, thus overcoming Shockley-Queisser limitations [1]–[3]. The QDs can be used in solar cells (SCs) to introduce Fermi quasi-levels between the valence band (VB) and the conduction band (CB), the so-called intermediate band (IB), to substantially improve the photovoltaic conversion efficiency (PCE). This technology has been named intermediate band solar cells (or *p-i-n* type

SCs), and they are classified within third generation SCs, as well as the tandem SCs, hot carriers, sensitized SCs, among others.

The *p-i-n* type SCs have generated great interest, being those parameters as the short circuit current (I_{sc}) and open circuit voltage (V_{oc}) can be improved adjusting the QDs distribution and sizes [4]. According to this, the QDs growth process in semiconductors is such important because their effective band gap (E_g) depend on their sizes [5]. To this end, there are some methods that have been proposed to produce QDs in films or suitable matrices, for example, beginning with an amorphous matrix. One possible methodology is to induce the nucleation of nanocrystals using impurities or defects, such that the control of QDs size can be done by suitably selecting the processing parameters [6], [7]. Some examples are the Si QDs in amorphous silicon (α -Si) [8]–[10], or the Ge QDs in amorphous germanium (α -Ge) [11], [12].

To obtain relevant results is convenient to induce the Ge QDs crystallization in a α -Ge matrix using low temperature processes, which allow obtaining the retired QDs density, in order to improve the External Quantum Efficiency (EQE) in photovoltaics cells type *p-i-n* without exceeding the limits of material activation energy [13].

In this work, we study the characteristics of nano-films with germanium quantum dots on a α -Ge matrix by combining a process based on the magnetron sputtering technique and a post-grown annealing stage process at different temperatures and a post-grown stage in a nitrogen atmosphere containing 10% of hydrogen in volume.

II. EXPERIMENTATION

The α -Ge films were grown by the magnetron sputtering technique in an ultra-high purity (UHP) argon atmosphere at different temperatures, a reference film was grown at room temperature (referred as Ge-A), and the set was completed with samples grown in the range of 500 to 800 K. The α -Ge films were produced with a thickness of ~120 nm. The

subsequent films were grown at a temperature of 500 K (Ge-B), 600 K (Ge-C) and 800 K (Ge-D), for 50 minutes for the first two and 70 minutes for the last one, with a thickness of 60 nm. The post-grown annealing treatment was performed on the Ge-B, Ge-C and Ge-D samples at 800 K for 3.5 hours in an atmosphere of N_2 containing H_2 at 10% by volume.

The chemical composition of the samples was measured by Second Ion Spectroscopy (SIMS). The films refractive index was determined by ellipsometry measurements at the wavelength of 632.8 nm and the optical band gap by transmittance measurements. The structural characteristics were measured by X-ray diffraction (XRD). The electrical properties were performed by the Hall-van der Pauw method. To identify the presence of Ge clusters, the films were characterized by Raman scattering, with photoluminescence measurements at room temperature.

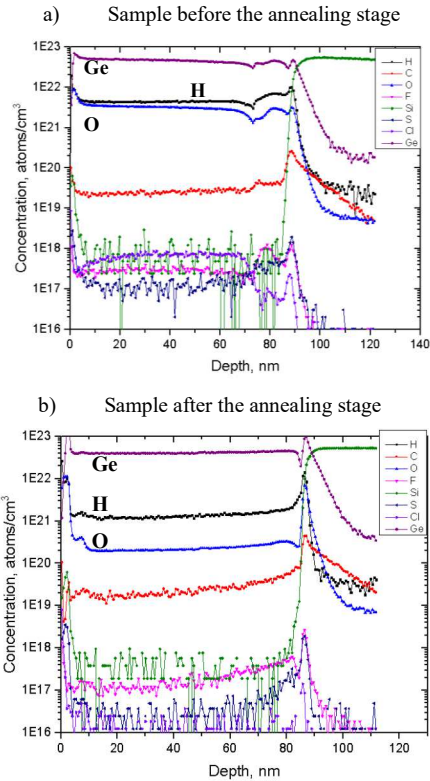


Fig. 1. Chemical composition analysis by SIMS of samples before (a) and after the annealing stage (b) at 800 K for 3.5 hours.

III. RESULTS AND DISCUSSION

The results of the chemical characterization of the nano-films by the SIMS technique are presented in figure 1. The data for the sample as they were grown are shown in fig. 1a), where an oxygen concentration of $\sim 4 \times 10^{21} \text{ cm}^{-3}$ is observed arising from the laboratory operative conditions. Therefore, the α -Ge nano-films contain 10% atomic of oxygen [GeO_x ($x \sim 0.1$)]. The oxygen concentration in the samples decreases after applying the annealing treatment by an order of magnitude. This oxygen reduction is explained by the presence of hydrogen in the atmosphere used during the post-grown annealing.

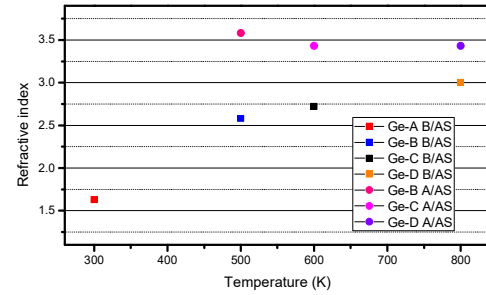


Fig. 2. Refractive index vs growth temperatures of Ge films before (B/AS) and after (A/AS) the annealing stage.

Figure 2 shows the measured refractive index for the different nano-films, as they were grown (B/AT) and the films that were applied annealing treatment at 800 K for 3.5 hours (A/AT). For the data interpretation, it must be noted that the crystalline Ge refractive index is 5.47 [14] and 1.9 for amorphous Ge [15] at 632.8 nm. According to Fig. 2, the sample grown at room temperature resulted amorphous. After applying the annealing stage, the refractive index for the films grown at temperatures higher than 500 K is about 3.5, suggesting the QDs formation, but the amorphous phase matrix remains.

TABLE I. RESULTS OF THE HALL-VAN DER PAUW MEASUREMENTS TO SAMPLES BEFORE AND AFTER THE ANNEALING STAGE.

Sample	Resistivity Ω/cm	Mobility $\text{Cm}^2/\text{V}\cdot\text{s}$	Concentration e/cm
Ge-D B/AS	0.413	5.978	$2.5\text{E}18$
Ge-B A/AS	0.024	11.2	$2.31\text{E}19$
Ge-C A/AS	0.012	9.6	$5.44\text{E}19$
Ge-D A/AS	0.021	10.4	$2.77\text{E}19$
α -Ge [14]	300	0.1	$1\text{E}18$

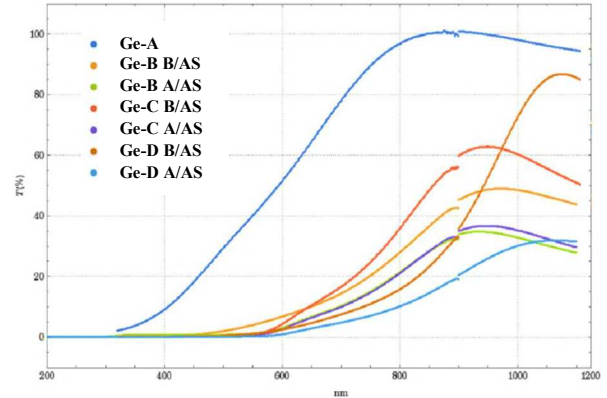


Fig. 3. Transmittance measurements to: sample as grown amorphous (Ge-A), grown at 500 K (Ge-B), 600 K (Ge-C) and 800 K (Ge-D), before (B/AS) and after the annealing treatment (A/AS).

To verify the films functionality for electronic devices, the electrical properties were measured and included in Table 1. The films grown at room temperature are electrically insulating. The set of samples that were subjected to the annealing stage resulted n-type, with high electron mobility, suggesting good structural quality and carrier concentration of $2.7 \times 10^{19} \text{ cm}^{-3}$ in average, consistent with their measured resistivity. For comparison purposes, the data on the electrical

properties of amorphous Ge samples reported in reference [14], are included. Although the values measured for this class of samples are equivalent to the data reported in the literature, it is necessary to determine the effect produced by the presence of oxygen in the samples.

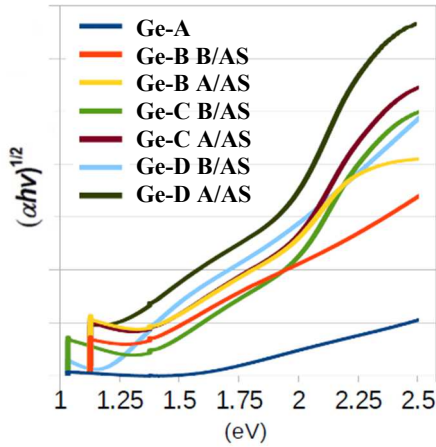


Fig. 4. Band Gap obtained by transmittance of Ge films before (B/AS) and after the annealing stage (A/AS) at 800 K for 3.5 hours.

The transmittance measurement was done on the different films, before and after the annealing stage. The sample grown at room temperature, amorphous Ge reference, has the highest transmittance, the films grown with temperature experience a decrease in transmittance after the annealing treatment. This decrease is related to the high carrier concentration and an increase in the degree of crystallinity in the samples.

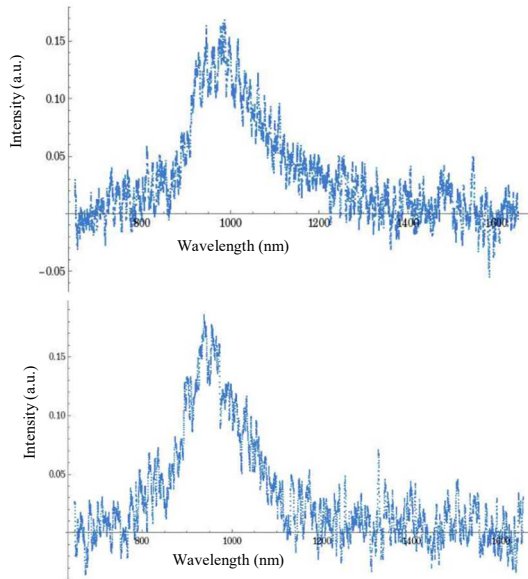


Fig. 5. Photoluminescence measurements to sample Ge-D at room temperature (the top) and a low temperature at 30 K (the bottom), after the annealing stage.

From the derivative of transmittance, the optical band gap of the films with the Ge clusters and the amorphous Ge reference sample was obtained. In figure 4, we observe the average optical E_g of the films is 1.2 eV. The band gap of the

Ge in bulk is located of the near infrared (0.6 eV), now the films grown at temperatures higher 500 K can absorb a larger range of photons, bringing us closer to the optimal E_g for a photovoltaic solar cell of 1.6 eV. Considering these characteristics is convenient grow films at temperatures above 500 K.

To confirm the data obtained by transmittance, we realized photoluminescence (PL) measurements and the results are show in the figure 5. The PL response presents signals clearly visible at ~ 1000 nm for the samples with the annealing treatment, this means that the films optic band gap is 1.2 eV. The PL response are more intensity in the samples grown at 800 K, which indicates that in these samples there are a higher degree of crystallinity by the possible formation of Ge clusters in an amorphous germanium matrix according to the refractive index data.

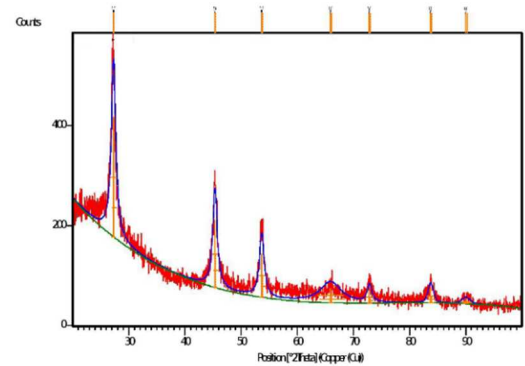


Fig. 6. X-ray pattern of sample Ge-D after the annealing treatment.

The films characteristics by X-ray diffraction confirm the last results. The X-ray pattern of the Ge-D sample after the annealing treatment is shown in Figure 6, where we observe the peaks corresponding to the crystalline Ge. It is worth mentioning that the samples without annealing do not present a visible x-ray signal because they are amorphous yet. Table 2 shows the results obtained from the XRD of the Ge-D sample before and after the annealing treatment. We observe that the diameter of the crystal is less than 1 nm for the sample before the annealing treatment, this corroborates why the no X-ray signal was obtained, and once the annealing is done, the size is between 6 and 8 nm. To confirm the presence of the clusters with nanometers size we measured the Raman spectra to the films, the results are present in figure 7.

TABLE II. XRD RESULTS TO SAMPLE GROWN AT 800 K (GE-D) BEFORE AND AFTER THE ANNEALING STAGE AT 800 K FOR 3.5 HOURS.

Pos. [°2Th.]	Height [cts]	FWHM Left [°2Th.]	d-spacing [Å]	Crystallite Size only [Å]	Micro Strain only [%]
Before the annealing stage					
26.83	729	7	3.32886	8.532735	19.50643
48	406	9	1.89469	10.57671	8.95688
51.5	188	6.9	1.77638	9.702609	9.154155
After the annealing stage					
27.28	238	0.96	3.26649	64.60409	2.528085
45.3	135	0.92	2.00038	68.8501	1.452709
53.61	86	0.97	1.70808	68.72669	1.242664

The Ge-D sample before and after the annealing stage was studied by the Raman spectroscopy, which helps us to confirm the presence of nanometers size crystals, according to the literature, the crystalline Ge signal is at 298 cm^{-1} and the intensity of the signal increases according to the crystallinity [16] whereas for the amorphous Ge the Raman signal is observed at 270 cm^{-1} [17]. This signal depends on the crystallinity of Ge, as shown by B. Zang *et al.* where they report the coexistence of Ge NCs and amorphous Ge in a SiO_2 matrix in samples grown from 350°C and as the temperature increases, the crystallinity increases notably up to 445°C .

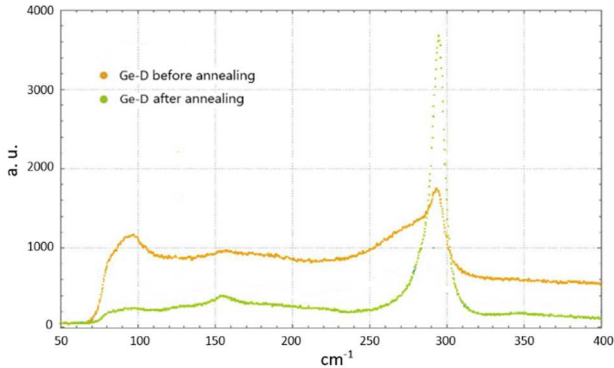


Fig. 7. Raman scattering spectra on the sample Ge-D before and after the annealing stage at 800 K for 3.5 hours.

The figure 7 shows the Raman spectra taken from the Ge-D sample before and after the annealing stage, grown at 800 K . The Ge-D samples before and after the annealing treatment find their maximum peak at the same position, this indicates a crystallinity ordering in both samples according to the Ref. [18]. When the annealing treatment is giving to the sample, we observed that the signal increases and decreases full width at medium intensity (FWHM), this indicates of the crystallinity in the material as mentioned in the Ref. [5]. According to the literature, a peak intensity change indicates a NC size increase in an amorphous matrix. Also, the annealing treatment process in combination with a suitable atmosphere produces the Ge clusters in an amorphous matrix [19].

IV. CONCLUSIONS

Amorphous Ge (α -Ge) nano-films containing Ge nanoclusters or quantum dots (QDs) with sizes in the range between 6 to 8 nm were grown by a combined process based on magnetron sputtering and a post-grown annealing at 800 K . The α -Ge matrix films grown by the magnetron sputtering technique resulted of n-type conductivity containing an atomic oxygen concentration of $\sim 10\%$, with electrons concentrations in the order of $\sim 2 \times 10^{19}\text{ cm}^{-3}$, carrier mobility of $10\text{ cm}^2/\text{V}\cdot\text{sec}$. The α -Ge films grown under ambient temperature conditions are insulating due to its amorphous nature and the operating conditions of the sputtering system, in particular the existence of minute amounts of oxygen in the grown chamber walls. The chemical composition measurements by the SIMS technique, allowed to show that the annealing treatment reduces the oxygen concentrations in

the samples. The post-grown annealing process applied to the nano-films in an atmosphere containing small amounts of hydrogen allowed to induce the formation of Ge nanocrystals. The annealing stage applied to the films causes the formation of Ge clusters in the GeO_x matrix. The refractive index increases consistently from 1.5 up to 3.5 when the samples were annealed at high temperature, suggesting the presence of germanium nanoclusters in the amorphous matrix. It was observed a reduction in the transmittance of the nano-films after the annealing treatment, this concerns with the high concentration of charge carriers, in addition to the change in the refractive index. Raman scattering measurements confirm the presence of Ge crystals in the films after the annealing treatment within the initial amorphous phase.

ACKNOWLEDGMENT

The author wishes to acknowledge M. Sc. Miguel Galván Arellano and Norma González García for their technical assistance and the films deposition by sputtering, at the Centro de Investigación y de Estudios Avanzados del Instituto Politécnico Nacional, México.

REFERENCES

- [1] A. J. Nozik, "Multiple exciton generation in semiconductor quantum dots," *Chem. Phys. Lett.*, vol. 457, pp. 3–11, 2008.
- [2] W. Shockley and H. J. Queisser, "Detailed balance limit of efficiency of p-n junction solar cells," *J. Appl. Phys.*, vol. 32, no. 3, pp. 510–519, 1961.
- [3] A. Luque and A. Martí, "Increasing the Efficiency of Ideal Solar Cells by Photon Induced Transitions at Intermediate Levels," *Phys. Rev. Lett.*, vol. 78, no. 26, pp. 5014–5017, 1997.
- [4] V. Aroutiounian, S. Petrosyan, A. Khachatryan, and K. Touryan, "Quantum dot solar cells," *J. Appl. Phys.*, vol. 89, no. 4, pp. 2268–2271, 2001.
- [5] S. Cosentino *et al.*, "Light harvesting with Ge quantum dots embedded in SiO_2 or Si_3N_4 ," *J. Appl. Phys.*, vol. 115, no. 4, 2014.
- [6] P. Germain, K. Zellama, S. Squelard, J. C. Bourgoin, and A. Gheorghiu, "Crystallization in amorphous germanium," *J. Appl. Phys.*, vol. 50, no. 11, pp. 6986–6994, 1979.
- [7] F. C. Li *et al.*, "Amorphous–nanocrystalline alloys: fabrication, properties, and applications," *Mater. Today Adv.*, vol. 4, p. 100027, 2019.
- [8] Y. Cao, P. Zhu, D. Li, X. Zeng, and D. Shan, "Size-dependent and enhanced photovoltaic performance of solar cells based on si quantum dots," *Energies*, vol. 13, no. 18, pp. 1–11, 2020.
- [9] D. K. R. Rai, N. R. Mavilla, A. K. Panchal, and C. S. Solanki, "Improvement in short circuit current of p-i-n solar cell with silicon quantum dot superlattice structure by optimizing SiNx thickness," *Conf. Rec. IEEE Photovolt. Spec. Conf.*, pp. 810–814, 2012.
- [10] A. Kole and P. Chaudhuri, "Growth of silicon quantum dots by oxidation of the silicon nanocrystals embedded within silicon carbide matrix," *AIP Adv.*, vol. 4, pp. 0–12, 2014.
- [11] D. Lehninger, J. Beyer, and J. Heitmann, "A Review on Ge

- Nanocrystals Embedded in SiO₂ and High-k Dielectrics,” *Phys. Status Solidi A*, vol. 1701028, pp. 1–13, 2018.
- [12] S. Mirabella *et al.*, “Matrix role in Ge nanoclusters embedded in Si₃N₄ or SiO₂,” *Appl. Phys. Lett.*, vol. 101, p. 011911, 2012.
- [13] A. Alguno *et al.*, “Enhanced quantum efficiency of solar cells with self-assembled Ge dots stacked in multilayer structure,” *Appl. Phys. Lett.*, vol. 83, no. 6, p. 1258, 2003.
- [14] D. E. A. and A. A. Studna, “Dielectric functions and optical parameters of Si, Ge, GaP, GaAs, GaSb, InP, InAs, and InSb from 1.5 to 6.0 eV,” *Phys. Rev. B*, vol. 27, no. 2, pp. 985–1009, 1983.
- [15] D. Lehninger *et al.*, “Ge Nanostructures Embedded in ZrO₂ Dielectric Films for Nonvolatile Memory Applications,” *ECS Trans.*, vol. 66, no. 4, pp. 203–212, 2015.
- [16] O. Salihoglu, U. Kürüm, H. G. Yaglioglu, A. Elmali, and A. Aydinli, “Crystallization of Ge in SiO₂ matrix by femtosecond laser processing,” *J. Vac. Sci. Technol. B*, vol. 30, no. 1, p. 011807, 2012.
- [17] B. Zhang, S. Shrestha, M. A. Green, and G. Conibeer, “Size controlled synthesis of Ge nanocrystals in SiO₂ at temperatures below 400°C using magnetron sputtering,” *Appl. Phys. A Mater. Sci. Process.*, vol. 96, no. 2010, p. 261901, 2012.
- [18] V. A. Volodin, D. V. Marin, V. A. Sachkov, E. B. Gorokhov, H. Rinnert, and M. Vergnat, “Applying an improved phonon confinement model to the analysis of Raman spectra of germanium nanocrystals,” *J. Exp. Theor. Phys.*, vol. 118, no. 1, pp. 65–71, 2014.
- [19] X. Zhu, G. H. Ten Brink, S. De Graaf, B. J. Kooi, and G. Palasantzas, “Gas-Phase Synthesis of Tunable-Size Germanium Nanocrystals by Inert Gas Condensation,” *Chem. Mater.*, vol. 32, no. 4, pp. 1627–1635, 2020.